A cement bond evaluation method based on the full waveform from a monopole tool

Hua Wang, Mike Fehler,Earth Resources Lab,Massachusetts Institute of Technology,Cambridge, MA, USA*

Summary

We use a 3D Finite Difference (3DFD) method to simulate monopole wavefields in a singly-cased borehole with different bonding conditions. Modal dispersion curves and dispersion analysis facilitate the identification of propagation modes. We find that the casing modes are strong when interface I (interface between casing and cement) is partially or fully replaced with fluid. The amplitude dependence on fluid thickness is small which could lead to ambiguity in interpretation. The casing modes are different when interface II (interface between cement and formation) is partially replaced with fluid, because the modes propagate in the mixed material of steel pipe and cement and the velocities are highly dependent on the cement thickness. It would highly possibly misjudge cement quality because the amplitudes of these modes are very small and they propagate with nearly the formation P velocity. However, it is possible to use the amplitude to estimate the thickness of the cement sheath because the variation of amplitude with thickness is very clear. While the Stoneley mode (ST1) propagates in the borehole fluid, a slow Stoneley mode (ST2) appears in the fluid column outside the casing when cement is partially or fully replaced with fluid. The velocity of ST2 is sensitive to the total thickness of the fluid column in the annulus independent of the location of the fluid relative to the cement. By combining measurements of the first arrival amplitude and ST2 velocity, we propose a full waveform method that can be used to eliminate the ambiguity and improve cement evaluation compared to the current method that uses only the first arrival

Introduction

Currently, the most commonly used method for evaluating cement quality is the CBL/VDL, which is based on the relationship between the fluid column thickness and the amplitude of the casing wave (e.g. Jutten and Corrigall, 1989; Liu et al., 2011; Wang et al., 2016), or/and on the arrival time (Zhang et al., 2011) of the first arrival. Measurements made on the first arrival can be ambiguous because of the small amplitude of the first arrival. In particular, if interface I is not cemented, the CBL/VDL cannot tell the bonding condition of interface II. Therefore, it is beneficial to study the wavefields in the single casing situation to determine the possibility of evaluating the bonding condition by using full waveforms. Although a number of studies have been conducted for single casing strings (e.g. Tubman et. al., 1984; Zhang et. al., 2011), the understanding of the wavefields in the single casing model is still incomplete. In this paper, we use a 3DFD (Wang et al., 2015) to simulate the monopole wavefield in single casing models with different bonding conditions. We attempt to understand if we can identify a relationship between fundamental mode propagation and the condition of the cement bonds.

Model

A singly-cased borehole model consists of multiple concentric cylinders. The innermost cylinder is the borehole fluid and the second is the steel pipe (or casing). The outermost cylinder is the formation (e.g. sandstone in Table 1). The material filling the annulus between the steel pipe and formation is cement. The cement may be partially or fully replaced with fluid. Table 1 lists the geometries and elastic parameters of an example fully cemented cased hole. In this study, we only change the geometry and filling material of the cement annulus to investigate the effect of different bonding conditions on full waveforms.

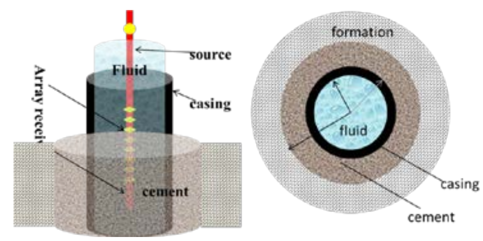

Figure 1 A good cemented model. Left is perspective view and right is the top-down view.

Table 1 Elastic parameters for the model used in our study.

Medium	Vp (m/s)	Vs (m/s)	Density (kg/m^3)	Radius(mm)
Fluid	1500	0	1000	108
Steel	5500	3170	8300	122
Cement	3000	1730	1800	170
Sandstone	4500	2650	2300	300

In the following sections, we discuss the wavefields of partially cemented models to determine the possibility of evaluating the bonding condition by using the full waveforms rather than the current method based on the first arrival (e.g. Walker, 1968; Zhang et al., 2011). By investigating the detail of the wavefields for models with different thicknesses of fluid and cement, we hope to get a direct method to determine the bonding condition including that between the outer casing interface and the formation by using data acquired by a commonly used array acoustic logging tool with a source having sonic frequencies (e.g. Zhang, et al., 2011).

Numerical simulations and analysis

Fluid between steel casing and cement

We first consider models in which interface I is filled with fluid. We investigate the wavefields in the models with the fluid thickness of 0 mm (fully cemented), 0.5 mm, 1 mm, 2 mm, 4 mm, 8 mm, 16 mm, 32 mm, 40 mm, and 48 mm (no cement) next to the casing. We calculate the modal dispersion curves for the models (Tubman et al., 1984; Zhang et al., 2016) and find that the ST2 (a slow Stoneley, e.g. Marzetta and Schoenberg, 1985) and casing modes vary with the fluid thickness (as shown in Figure 2) while other modes such as ST1 (Stoneley in borehole) and pR (pseudo Rayleigh) have no change. Figure 2a shows the dispersion curves for ST2 with various fluid thicknesses. We find the ST2 mode is very sensitive to fluid thickness. The velocity of ST2 increases with the fluid thickness. This means that the velocity of ST2 could be a good indicator for cement bond evaluation.

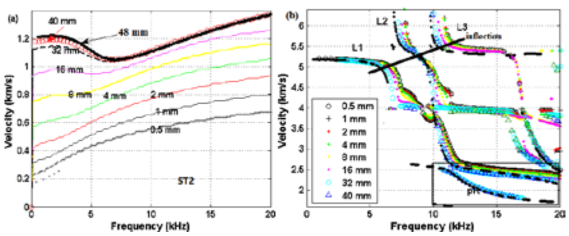

Figure 2 Dispersion curves of ST2, L and pR modes with various fluid thicknesses at interface I.

There is a very small difference in velocity of the L modes with fluid thicknesses (Figure 2b). The black dotted lines, denoting the modes in case of the fluid thickness of 48 mm, are almost the same as the modes in the cases with partial cement except at the lower frequencies at the inflection points (marked with a solid line) for different L modes.

We simulate the full waveforms for most of the models (fluid thickness of 0 mm, 4 mm, 8 mm, 16 mm, 32 mm, 40 mm, and 48 mm) as shown in Figure 3 (traces for source-receiver spacing of 3 m are shown). In Figure 3a, we see the clear casing mode as the first arrival when the cement is partially replaced with fluid. Walker (1968) was the first to give the relationship between the amplitude of the casing modes and the thicknesses of cement sheath. The current methods for cement evaluation are mostly based on his relationship. However, the small dependence of the amplitude of the first arrival with fluid thickness, shown in Figure 3a, challenges the tool design and data processing.

The P wave is submerged in the casing modes and cannot be discerned which is similar to the case of P wave measurements in the fast-fast formations in acoustic logging-while-drilling situations (Wang et al., 2017). The difficult to discern arrival time of S wave makes the velocity measurement difficult when fluid exists. The ST1 and ST2 modes are hard to discern due to the strong interference from pR. Figure 3b shows traces that have been filtered using a 5 kHz to 8 kHz band filter. It is easy to identify ST1 and ST2 in the waveforms although the ST2 is not clear when the fluid thickness is 4 mm and 8 mm. The small velocity of ST2 suggests that a large offset would be helpful to separate the ST1 and ST2 for the small fluid thickness cases. The velocity analysis in time (Kimball and Marzetta, 1984) (based on the filtered data) and frequency domains for the case with the fluid thickness of 16 mm are given in Figure 4

We easily find casing, S and pR, ST1, and ST2 modes from the velocity-time semblance plot (Figure 4a). In Figure 4b, we plot the modal dispersion curves using dotted lines on the dispersion analysis contour plot (Wang et al., 2015) obtained from the array waveforms. The match between the modal dispersion curves and dispersion analysis plot for different modes is very good, especially for the ST modes. The velocity analyses illustrate the possibility using the later part of the waveform to determine the fluid thickness at interface I rather than the relatively small amplitude of the first arrival. If we find casing modes, we can consider interface I is filled with fluid and then we can use the ST2 to determine the thickness of the fluid column.

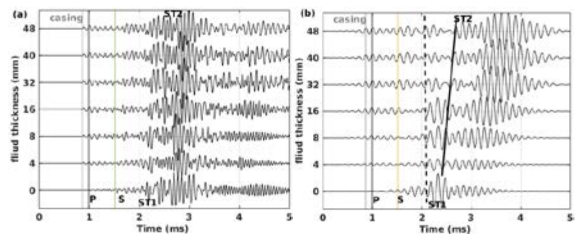

Figure 3 Synthetic waveforms for the models with the fluid of various thicknesses at interface I.

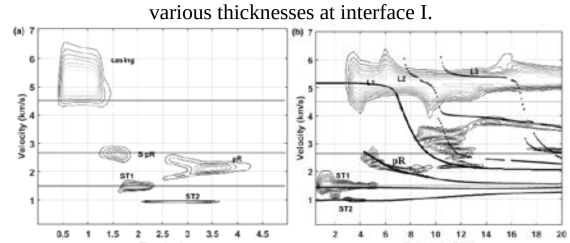

Figure 4 Velocity analysis in time and frequency domains for the synthetic waveforms with the fluid thickness of 16 mm (the source-receiver spacing is 2.6 m, and the interval is 0.2 m).

Fluid between cement sheath and formation

It is very critical to evaluate the bonding condition of interface II because it is close to the reservoir or aquifer. Here we investigate the models with some of the cement being replacing with fluid. We will not display the modal dispersion curves for the models here because the characteristics are similar to those in Figure 2 for interface I. There are L, pR, ST1, and ST2 modes. The only difference is the lower speed of the L modes and the shifting of the inflection points to lower frequency. Here the L modes propagate in a mixed material of steel pipe and cement with the slower speeds since they no longer only propagate in the steel pipe. The cement next to casing enlarges the effective radius of the pipe and moves the inflection points to lower frequencies. The trend of the dispersion curves of these modes is that with more cement, velocity decreases and the inflection point shifts towards lower frequency. We cannot find any difference in dispersion for mode ST2 from that shown in Figure 2a for the corresponding fluid thickness cases. This suggests that ST2 cannot be used as an indicator for the location of where the fluid column exists. However, at a minimum, we can know whether interface II is bonded well by using the arrival time and velocity of the L modes (Zhang et al., 2011). Then we can determine the thickness of the fluid column next to the formation by using the ST2 mode.

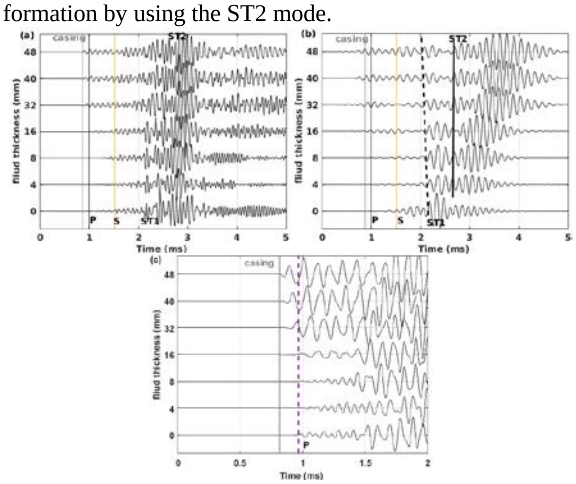

Figure 5 Synthetic waveforms for models with the fluid of various thicknesses at interface II. (source-receiver spacing of 3 m). (a) Original waveforms. (b) waveforms that have been filtered with a band pass filter from 5 kHz to 8 kHz. (c) Unfiltered waveforms from 0 to 2 ms of (a).

We display the full waveforms in Figure 5 in the same manner as Figure 3. In the detailed display of the waveforms in Figure 5c, we see a clear casing mode (a combination of casing and cement modes) as the first arrival between the labeled casing and P arrivals when the cement is partially replaced with fluid. Although the P wave is submerged in the mode and cannot be discerned when the fluid column is large, the mode propagates with the P velocity when the thickness of fluid column is as small as 4 mm to about 16 mm and its presence could be interpreted as indicating good cement. Fortunately, we find a clear ST2 in the waveforms, especially those that have been filtered (Figure 5b), which can help us avoid the misinterpretation. Similar to the case of interface I, we suggest the use of a large offset to separate the ST2 modes for the thin (4 mm to 8 mm) fluid column. Figure 6 shows the velocity-time semblance (Figure 6a) and dispersion analysis (Figure 6b) plots for a model with 16 mm fluid column at interface II. From Figure 6a, we clearly find a casing-cement mode with a velocity nearly the same as the P velocity in addition to S, ST1, ST2 modes. As mentioned, if we only use the first arrival to determine the bonding condition, we will definitely misjudge the bonding condition as indicating very good cement even for the fluid column thickness of 16 mm at interface II. However, the good coherence for ST2 (from the filtered waveforms) in Figure 6a gives us an opportunity to avoid the misjudgment. The dispersion analysis plot in Figure 6b gives us another view for mode identification which can also be used to eliminate the misjudgment. The modal curves (dotted lines) for the model with fluid column thickness of 16 mm at interface I is also plotted to illustrate the difference from Figure 4b. We find the dispersion characteristics of pR, ST1, and ST2 are the same as those in Figure 4b. The casing-cement modes, which will likely be identified as P waves, have slower velocities than the P wave and the L modes in Figure 4b.

Our results show that it is necessary to use the full waveform, especially the later part of the waveforms, to estimate the cement bonding condition when a fluid column exists at interface II. A large offset receiver is necessary to make the ST2 visible. In field applications, dispersion analysis may be impractical due to the time it requires. Time semblance would be also helpful because we could get velocity information about the ST2 mode which can be a very good indicator for bad bonding condition. Cement evaluation will be highly improved by using the full waveform.

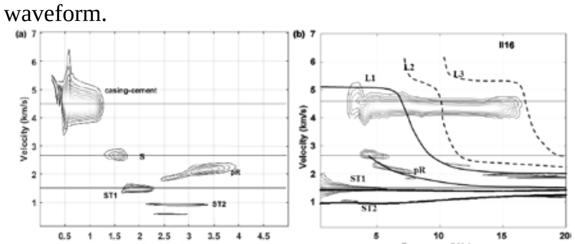

Figure 6 Velocity analysis in time and frequency domains for synthetic waveforms with the fluid thickness of 16 mm at interface II.

Cement inside the fluid columns

To give more detail about the relationship between the waveforms and the thickness and location of the fluid column and cement sheath, we separate the annulus between casing and formation into three parts with each part being a different medium (cement or fluid) with different thickness. We simulate the waveforms in models with cement partially replacing fluid columns at both interfaces I and II. All the waveforms are shown in Figure 7a and the names for different models are also listed on the waveforms. The letters 'f' and 'c' are fluid and cement, respectively. The number before the letter is the thickness (units in mm) of the medium. For example, '4f16c28f' means the annulus consists of 4 mm and 28 mm fluid columns at interfaces I and II, respectively. In addition, a 16 mm thick cement layer is placed between the two fluid columns. The arrival times for different modes are marked by lines. Because a fluid column exists at interface I, the arrival time of the casing mode is the same independent on the thickness of the fluid column. The amplitude of the casing wave changes a little with the changing thickness of the fluid next to the casing. The current cement bonding evaluation method is based on the relationship between the amplitude of the casing wave and the fluid column thickness (e.g. Jutten and Corrigall, 1989; Liu et al., 2011). However, this method strongly depends on measurements of the amplitude of the first arrival and could lead to misinterpretation because the amplitude dependence on fluid column thickness is not strong. Another issue is that we cannot infer the bonding condition of interface II if interface I is partially replaced with fluid.

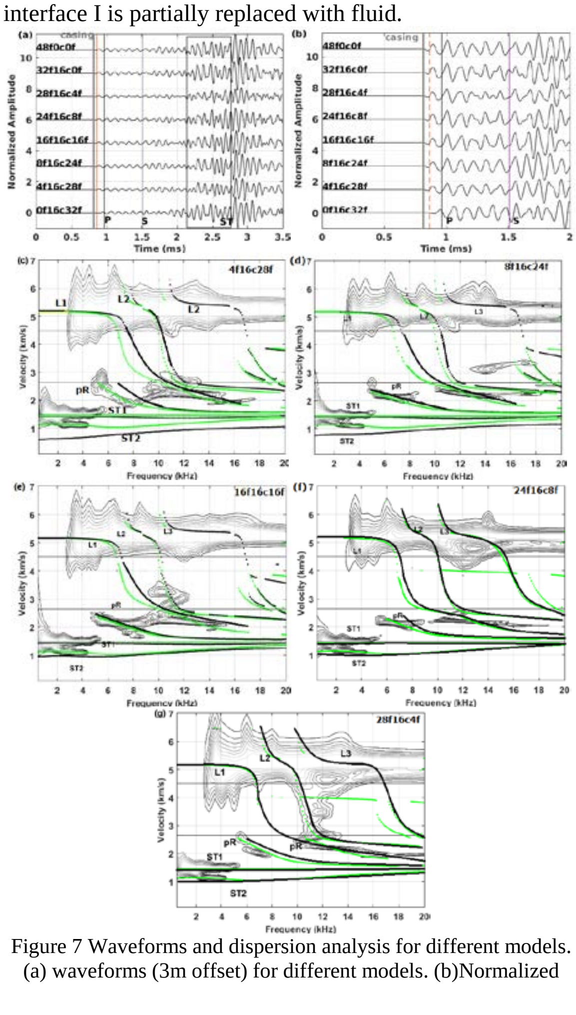

Figure 7 Waveforms and dispersion analysis for different models. (a) waveforms (3m offset) for different models. (b)Normalized waveforms of the first 2 ms. (c)-(g) dispersion analysis plots for the waveforms in different models.

We also find little difference in the ST waves (inside the rectangle in Figure 7a) with fluid thickness. The casing, P, and S waves are expanded and shown in Figure 7b.The dispersion analysis (contour) plots for the waveforms from different models are shown in from Figures 7c to 7g. The green lines are the dispersion curves for a model with a 32 mm fluid column at interface I (Figure 2). The black lines are the dispersion curves for a model with fluid at interface I (Figure 2) of 4 mm (Figure 7c), 8 mm (Figure 7d), 16 mm (Figure 7e), 24 mm (Figure 7f) and 28 mm (Figure 7g). It is obvious that the green lines for mode ST2 match the dispersion contour plots for all fluid column thicknesses. This suggests that the ST2 wave can be used to determine the total thickness of the fluid column in the annulus and it is not just sensitive to the fluid thickness next to the casing if there is another fluid column between cement and formation. This may be considered to be a limitation of the application of the ST2 wave. However, it would be a great supplement for the current first arrival amplitude method. We can use the amplitude of the casing wave to determine the fluid thickness next to the casing although sometime this method will not work very well. We can get the total fluid thickness in the annulus by comparing the velocity or dispersion curves with the modal cases. Then we can know the distribution of the fluid in the annulus. This overcomes the limitation of the current amplitude method on the bonding condition of interface II and can also eliminate an ambiguous interpretation.

Conclusions

We have used a 3DFD method to simulate wave propagation from a monopole tool in a singly-cased borehole with different bonding conditions. Data processing methods such as velocity-time semblance and dispersion analysis facilitate the identification of the modes in the different models. Our conclusions are as follows,

(1) The small variation of first arrival amplitude with the thickness of fluid at interface I could introduce ambiguity in the interpretation of the first arrival method. It would be highly likely that the presence of fluid in the interface I would be misjudged as good cement.

(2) The slow Stoneley (ST2) mode can be used to evaluate the total thickness of the fluid column in the annulus independent on the fluid location.

(3) Analysis of the full waveform by combining the first arrival and the slow ST waves can be used to eliminate the ambiguity about cement condition and to improve cement evaluation reliability compared to the current method using only first arrival measurements

Acknowledgments

This study is supported by the Founding Members Consortium of the Earth resources Laboratory at MIT.

EDITED REFERENCES

Note: This reference list is a copyedited version of the reference list submitted by the author. Reference lists for the 2017 SEG Technical Program Expanded Abstracts have been copyedited so that references provided with the online metadata for each paper will achieve a high degree of linking to cited sources that appear on the Web.

REFERENCES

Jutten J., and Corrigall E., 1989, Studies with narrow cement thickness lead to improved CBL in concentric casings: Journal of Petroleum Technology, **11**, 1158–1192.

Kimball, C.V., and T. Marzetta, 1986, Semblance processing of borehole acoustic array data: Geophysics, **49**, 274–281, http://org/doi/abs/10.1190/1.1441659.

Liu X., Chen D., Chen H., and Wang X., 2011, The effects of the fluid annulus thickness at the first interface on the casing wave: Technical Acoustics, **30**, 301–305.

Marzetta, T. and M. Schoenberg, 1985, Tube waves in cased boreholes: 55th Annual International Meeting, SEG, Expanded Abstracts, 34–36, http://org/doi/abs/10.1190/1.1892647.

Tubman, K. M., Cole, S. P., Cheng, C. H., and Toksöz, M. N., 1984, Dispersion curves and synthetic microseismograms in unbonded cased boreholes: Earth Resources Laboratory Industry Consortia Annual Report, 1984-02.

Walker, T., 1968, A full-wave diplay of acoustic signal in cased holes, SPE 1751.

Wang, H., G., Tao, and M. C., Fehler, 2015, Investigation of the high-frequency wavefield of an off-center monopole acoustic logging-while-drilling tool: Geophysics, **80**, no.4, D329–D341. http://library.seg.org/doi/abs/10.1190/geo2014-0426.1.

Wang, H., G., Tao, and X., Shang, 2016, Understanding acoustic methods for cement bond logging, Journal of Acoustical Society of America, **139**, 2407–2416, http://dx.doi.org/10.1121/1.4947511.

Wang, H., M.C. Fehler, and D. Miller, 2017, Reliability of velocity measurements of monopole acoustic Logging-while-drilling tool in fast formations: Geophysics, (accepted).

Zhang, H., D., Xie, Z., Shang, X., Yang, H., Wang, and H., Tao, 2011, Simulated various characteristic waves in acoustic full waveform relating to cement bond on the secondary interface, Journal of Applied Geophysics, **73**, 139–154.

Zhang, X., Wang, X., and Zhang, H., 2016, Leaky modes and the first arrivals in cased boreholes with poorly bonded conditions: Science China-Physics, Mechanics & Astronomy, **59**, 624301.